Supplementary Information for

Biocompatible and Totally-Disintegrable Semiconducting Polymer for Ultrathin and Ultra-Lightweight Transient Electronics

Ting Lei[1], Ming Guan[2], Jia Liu[1], Hung-Cheng Lin[1], Raphael Pfattner[1], Leo Shaw[1], Allister F. McGuire[3], Tsung-Ching Huang[4], Lei-Lai Shao[5], Kwang-Ting Cheng[5], Jeffrey B. Tok[1], and Zhenan Bao[1,]*

[1]Department of Chemical Engineering, [2]Department of Materials Science & Engineering, [3]Department of Chemistry, Stanford University, Stanford, CA 94305, USA. [4]Hewlett Packard Labs, Palo Alto, CA 94304, USA. [5]Department of Electrical and Computer Engineering, University of California, Santa Barbara, CA 93106 USA.

[*]Correspondence and requests for materials should be addressed to Zhenan Bao (zbao@stanford.edu)

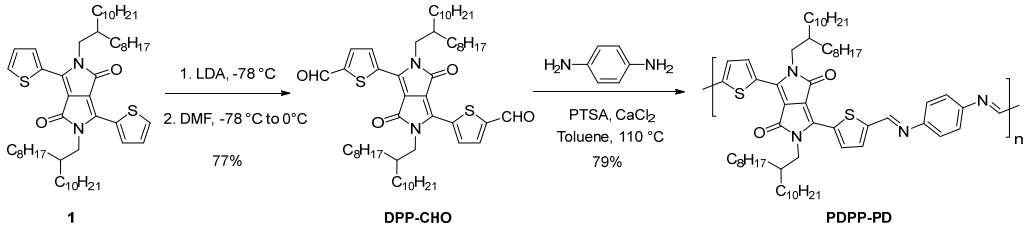

Scheme S1. Synthesis of the disintegrable polymers.

Materials

All reagents and starting materials were purchased from commercial sources and used without further purification. Compound 1 was synthesized according to the literature.[1] Cellulose (Sigmacell Cellulose Type 20), cellulase (from Trichoderma viride) and a pH-4.6 buffer solution (acetic acid-sodium acetate buffer, 1:1) were purchased from Sigma-Aldrich.

Polymer synthesis

5,5'-(2,5-bis(2-octyldodecyl)-3,6-dioxo-2,3,5,6-tetrahydropyrrolo[3,4-c]pyrrole-1,4-diyl)bis(thiophene-2-carbaldehyde) (**DPP-CHO**)[2]: To a 100 mL round bottom flask, diisopropylamine (0.98 mL, 6.96 mmol) and THF (50 mL) were added. *n*-BuLi (1.6 M, 2.9 mL, 4.64 mmol) was added and stirred at 0 °C for 30 min to prepare fresh lithium diisopropylamide (LDA). Compound **1** (1.0 g, 1.16 mmol) in THF (20 mL) was then added dropwise into the flask at −78 °C. After stirring at −78 °C for 30 min, dry DMF (0.46 mL, 6.96 mmol) was added dropwise at −78 °C. The mixture was allowed to warm up to room temperature and stir for 1 h. Then the mixture was quenched with 20 mL of water. The aqueous layer was extracted with dichloromethane (3 × 50 mL). The combined extracts were washed with distilled water and dried over anhydrous Na_2SO_4. After removal of the solvents under reduced pressure, the residue was purified by chromatography with silica (eluent: hexane/ ethyl acetate = 20/1 to 10/1) to afford **DPP-CHO** as a dark red solid. Yield: 0.82 g (77%). ^{1}H NMR ($CDCl_3$, 300 MHz, ppm): δ 10.03 (s, 2H), 9.04–9.02 (d, J = 4.2 Hz, 2H), 7.88–7.86 (d, J = 4.2 Hz, 2H), 4.05–4.03 (d, J = 7.7 Hz, 4H), 1.89–1.86 (m, 2H), 1.45–1.18 (m, 64H), 0.94–0.81 (m, 12H).

Polymerization for **PDPP-PD:** To a Schlenk tube (100 mL), **DPP-CHO** (250 mg, 0.273 mmol), *p*-phenylenediamine (29.5 mg, 0.273 mmol), *p*-toluenesulfonic acid (PTSA) (2.6 mg, 0.014 mmol, 5 mol%), anhydrous $CaCl_2$ (100 mg, drying agent), and anhydrous toluene (30 mL) were added under nitrogen atmosphere. The tube was then sealed under a nitrogen atmosphere. The mixture was stirred for 48 h at 110 °C. After completion, dry K_2CO_3 (10 mg) was added to neutralize the acid. The mixture was stirred at 110 °C for 30 min and then the filtered through a nylon filter to remove the drying agent and any insoluble salts. After removing the solvent in the filtrate, the polymers were purified via Soxhlet extraction for 2 h with dry acetone and 2 h with hexane, and was finally collected with chloroform. The chloroform fraction was then evaporated to remove the solvent and afford a dark green solid (213 mg, yield 79%). ^{1}H NMR ($C_2D_2Cl_4$, 400 MHz, 393 K, ppm): δ 10.07–10.05 (m, 2H), 8.95–8.67 (m, 3H), 7.89–7.67 (m, 2H), 7.40 (m, 1H), 7.26–7.24 (m, 1H), 6.76–6.74 (m, 1H), 4.15–4.07 (m, 4H), 2.06–2.19 (m, 2H), 1.51–1.32 (m, 64H), 0.96–0.93 (m, 12H).

Two conditions were used for preparing polymer PDPP-PD: (1) with drying agent $CaCl_2$. (2) without drying agent $CaCl_2$. The first condition provides higher molecular weight of (M_w/M_n = 39.6 kDa /15.0 kDa, PDI = 2.64) M_w: 39,574 Da, PDI: 2.64; while the second conditions provides lower molecular weight (M_w/M_n = 19.1 kDa /7.7 kDa, PDI = 2.48).

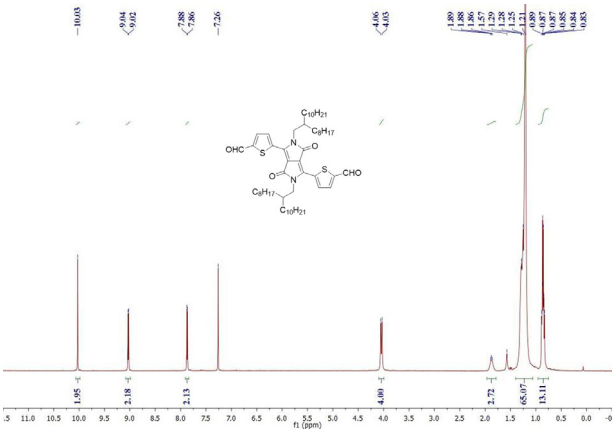

^{1}H NMR spectrum of DPP-CHO in $CDCl_3$ at 298K.

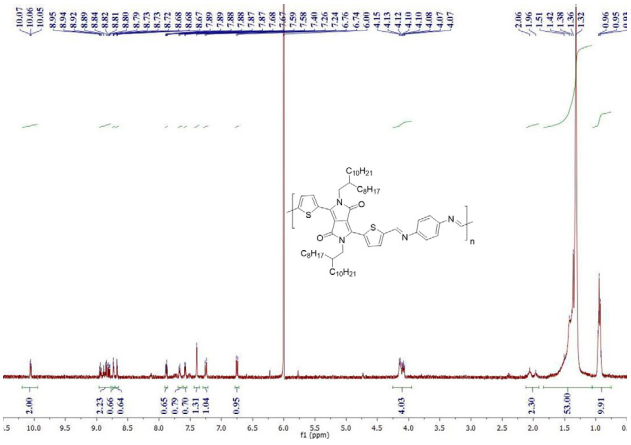

^{1}H NMR spectrum of polymer PDPP-PD in $C_2D_2Cl_4$ at 393K.

Synthesis of trimethylsilyl cellulose (TMSC)[3] TMSC was synthesized by suspending cellulose (2 g) in 9% LiCl/DMAc. The mixture was heated to 150 °C. After the cellulose completely dissolved, the solution was heated to 80 °C and 20 ml of HMDS was added in dropwise within one hour in a nitrogen atmosphere. The solution was stirred at 80 °C for 12 h. The mixture was cooled down and some methanol was added to precipitate the TMSC. The crystallized TMSC was filtered and washed several times with methanol and dried in vacuum.

Methods

High-temperature gel permeation chromatography (HT-GPC) was performed on Tosoh High-temperature EcoSEC (RI detector) at 180 °C using 1,2,4-tricholorobenzene (TCB) as the eluent.

Thermal gravimetric analysis (TGA) was performed using a Mettler Toledo TGA/SDTA 851e at a heating rate of 10 °C/min under nitrogen flow (20 mL/min).

Cyclic voltammetry (CV) was performed using a drop-cast polymer thin film on glassy carbon electrode. Acetonitrile containing 0.1 M *n*-Bu_4NPF_6 was used an electrolyte. All potentials were recorded versus Ag/AgCl as a reference electrode (scan rate: 50 mV s^{-1}).

Density functional theory (DFT) calculations were performed in Gaussian 09 D.01 program[4] using the B3LYP functional and 6-311G(d,p) basis set.

Cell viability tests. A glass substrate was used as the control substrate. The PDPP-PD film was spin-coated on glass substrate with a 100-nm thickness. Both samples were sterilized with UV exposure, and a 75% ethanol aqueous solution. After sterilization, samples were rinsed with phosphate-buffered saline (PBS) and then coated with 10 mg/mL fibronectin in a 0.02% w/w gelatin solution overnight. HL-1 cells were then plated inside the chamber at a density of 10^4 cells/cm^2 and maintained in Claycomb medium supplemented with a 10% fetal bovine serum, 0.1 mM norepinephrine, 2 mM L-glutamine and 100 U/mL penicillin and 100 mg/mL streptomycin in a 37 ºC incubator with 5% CO_2. The medium was changed daily. Cell viability was evaluated using a LIVE/DEAD® Viability/Cytotoxicity Kit (Molecular Probes, Invitrogen, Grand Island, NY). On 2, 4 and 6 days of *in vitro* culture, cells were stained by 1 mM calcein-AM and 1 mM ethidium homodimer-1 (EthD-1) for 30 min and then washed three times with PBS. Samples were imaged by an inverted microscope (Leica DMI6000 B).

Grazing-incidence X-ray diffraction (GIXD) was performed at the Stanford Synchrotron Radiation Lightsource at beamline 11-3 with a MAR CCD detector. The incident angle was 0.20°, which allows for probing throughout the complete thickness of the film while avoiding multiple reflection from the Si substrate (with native oxide). The beam energy was 12.73 keV, and the sample-to-detector distance was 300 mm. Samples were kept in a helium environment to minimize air scattering. Diffraction images were corrected to account for the planar detector. Linecuts along the horizon (q_z = 0) were calculated by integrating a q range of 0.01 $Å^{-1}$ around the polar angle χ = 90°. The meridian linecut (q_{xy} = 0) was not adjusted for detector planarity, and thus the q values of the x-axis are approximate for that curve. Lastly, the χ-integrated intensity was obtained by summing counts between χ = 0° and χ = 81°. Total intensity was shifted in Fig. S9 to fit on a single plot.

Polymer FET devices fabricated on Si/SiO_2 substrates. Top-contact/bottom-gate OFET devices were fabricated using n^+-Si/SiO_2 (300 nm) substrates where n^+-Si and SiO_2 were used as the gate electrode and gate dielectric, respectively. The substrates were subjected to ultrasonication in acetone, a cleaning agent, deionized water (twice), and isopropanol. The substrates were then treated by oxygen plasma for 2 min and transferred into a glove box. The substrates were modified with *n*-octadecyltrimethoxysilane (OTS) to form a SAM monolayer according to literature procedures.[3] Thin films of the polymer were deposited on the treated substrates by spin coating using a 5 mg/mL polymer solution in trichloroethylene (TCE), followed by thermal annealing at 150 °C under nitrogen. After the thin film deposition, 40-nm-thick gold were deposited as source and drain contacts using a shadow mask.

The evaluations of the OFETs were carried out in ambient using a Keithley 4200 parameter analyzer on a probe stage. The carrier mobility μ was calculated from the data in the saturated regime according to the equation $I_{SD} = (W/2L)C_i\mu(V_G - V_T)^2$.

Fabrication of the ultrathin cellulose film. Dextran (5% in DI water) was spin-coated on a carrier chip at 2,000 rpm for 60 s and subsequently baked at 150 °C for 10 min. TMSC in chlorobenzene (70mg/mL) was spin-coated at 2000 rpm for 60s with 100 °C annealing for 10 min. The film was then hydrolyzed in a95% acetic acid atmosphere for 2 h and annealed at 150 °C for 10 min. The TMSC spin-coating and hydrolyzation steps were repeated to obtain a thicker film of 800 nm.

Fabrication of totally disintegrable devices with iron electrodes. The fully disintegrable devices were fabricated using a procedure similar to that of the ultrathin disintegrable device. The metal gate, interconnects, and source-drain electrodes were replaced by thermal evaporation of 40-nm Fe. For the decomposition experiment, the devices were soaked in a 1 mg/mL cellulase buffer solution at room temperature. (cellulase from *Trichoderma viride*; sodium acetate/acetic acid buffer at pH 4.6). The polymer film thickness changes of the polymer films were monitored by profilometer and the thickness changes of the Al_2O_3 layer were measured by ellipsometer.

Supplementary Figures and Table.

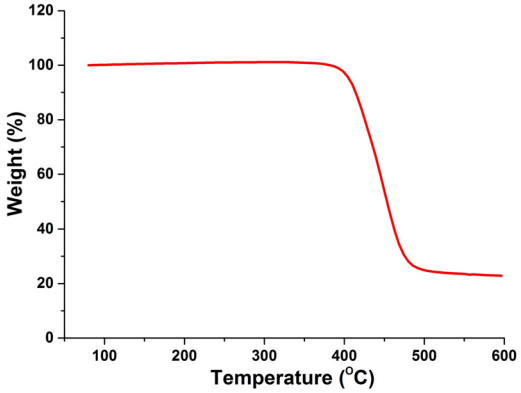

Figure S1| Thermogravimetric analyses (TGA) of PDPP-PD (5% loss at 404 °C).

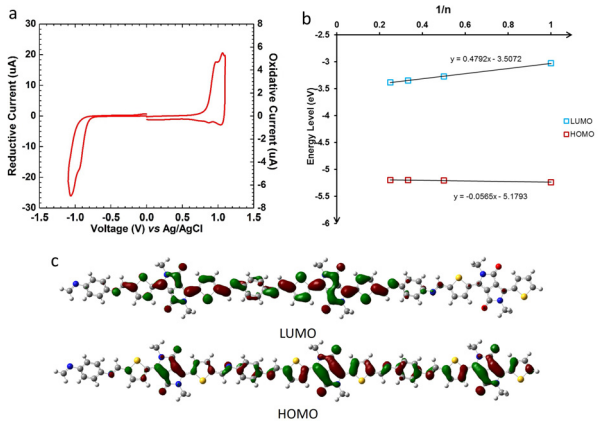

Figure S2| Experimental and DFT calculated electrochemical properties of PDPP-PD. **a**, cyclic voltammograms of PDPP-PD in drop-casted film. Measured E_{HOMO} = −5.11 eV, E_{LUMO} = −3.54 eV. **b**, HOMO and LUMO energy levels of PDPP-PD extrapolated from the values computed for its oligomers (n = 1, 2, 3, and 4) (B3LYP/6-311G(d,p)). Calculated E_{HOMO}^{Calc} = −5.18 eV, E_{LUMO}^{Calc} = −3.51 eV. c, calculated molecular frontier orbitals of the PDPP-PD trimer (B3LYP/6-311G(d,p)).

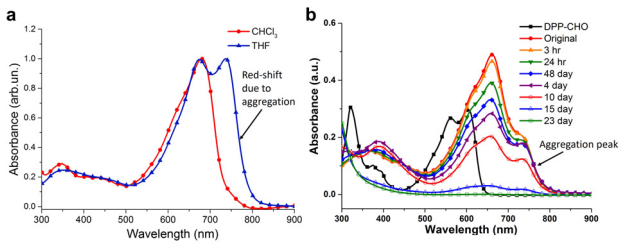

Figure S3| Characterization of polymer property in different solvents and the decomposition process in THF. **a**, Comparison of the polymer absorption in "good" ($CHCl_3$) and "poor" (THF) solvents. As indicated by the absorption spectra, the polymer shows an aggregation peak in THF; whereas in $CHCl_3$, the polymer is individualized by solvent molecules. **b**, Absorption spectrum changes in the decomposition process of PDPP-PD in THF. The decomposition was performed by adding 1% (v/v) acetic acid and 1% (v/v) DI water into the polymer THF solution. THF is a bad solvent for the polymer, as indicated by the polymer aggregation peak at 730 nm. Because of the polymer aggregation, the decomposition of the imine bonds (first step) becomes slower in THF. However, water has a much better solubility in THF, which accelerates the decomposition of the monomer DPP-CHO. Therefore, we did not observe the absorption feature of the monomer DPP-CHO. The polymer aggregation resulted in a different degradation process in "good" and "poor" solvents.

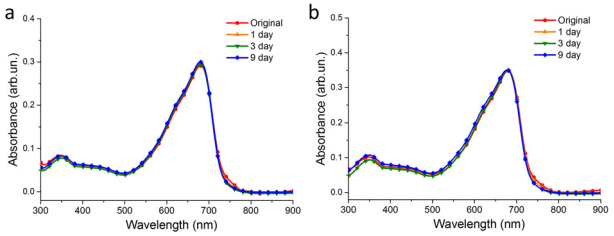

Figure S4| Stability test of PDPP-PD in a, neutral (1% v/v DI water) and b, basic (1% v/v $NH_3 \cdot H_2O$) conditions. The imine bond is stable in both neutral and basic conditions. We did not observe any significant degradation of the polymer in both neutral and basic conditions.

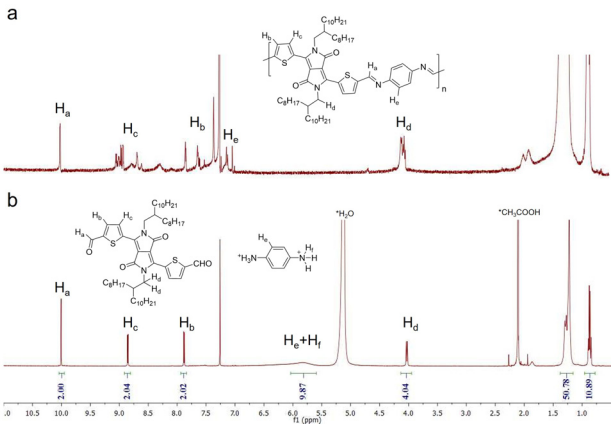

Figure S5| *In situ* NMR study of the decomposition process of PDPP-PD. ^1H NMR spectrum of polymer PDPP-PD (**a**) before and (**b**) after decomposition. The NMR was performed using $CDCl_3$ as a solvent at 60 °C. AcOH and water were added, as indicated by both the H_2O and AcOH peaks. Before polymer decomposition, the polymer showed multiple broad peaks in the aromatic region due to the strong aggregation of the polymer. After decomposition, the solution exhibited well-defined split peaks of DPP-CHO and the broad peak of *p*-phenylenediamine.

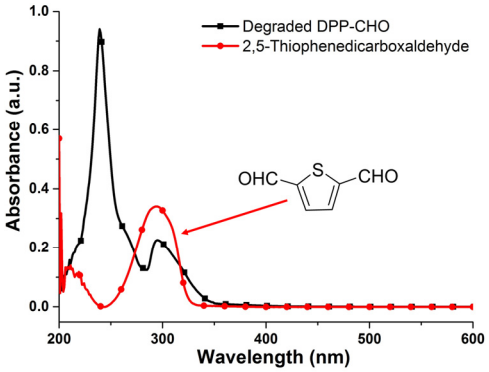

Figure S6| Comparison of the absorption spectra of degraded DPP-CHO and 2,5-thiophenedicarboxaldehyde. The absorption peaks of the degraded compound are in the UV region (< 350 nm), indicating that the degrade compound has smaller conjugation length compared to the 2,5-thiophenedicarboxaldehyde. We thus propose that the diketopyrrolopyrrole ring was decomposed under the acid conditions.

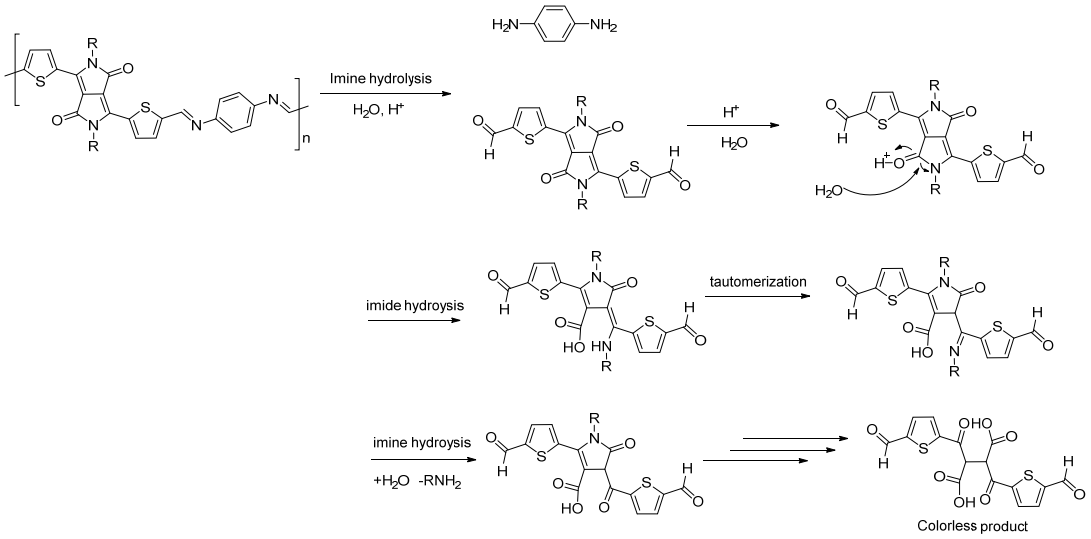

Figure S7| Proposed decomposition mechanism for PDPP-PD. The decomposition process contains two steps: (1) imine bond hydrolysis; (2) lactam ring hydrolysis.

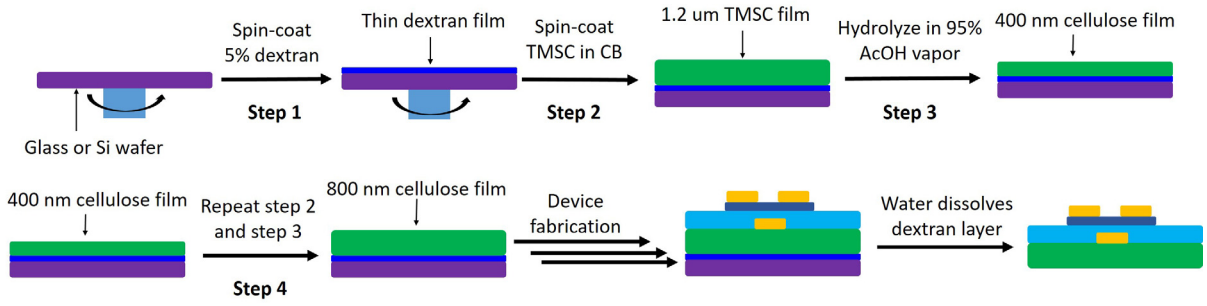

Figure S8| Schematic of the fabrication process for the 800-nm cellulose substrate.

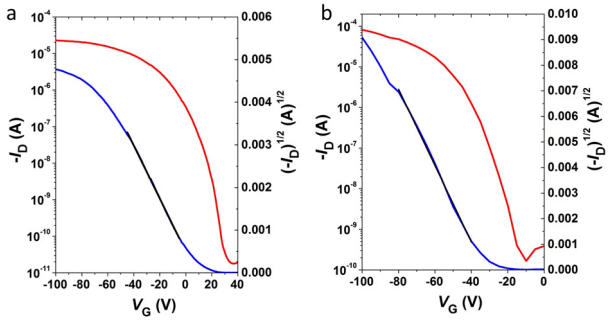

Figure S9| Comparison of the transfer characteristics of PDPP-PD with different molecular weights. a, Transfer characteristics of the low molecular PDPP-PD; mobility fitting range is from −5 to −45 V (black line). **b**, Transfer characteristics of the high molecular weight PDPP-PD, mobility fitting range is from −40 to −80 V (black line). The devices were fabricated on OTS-treated SiO_2 (300 nm)/n^{++}-Si substrate. (V_{DS} = −100V, L = 50 μm, W = 1000 μm).

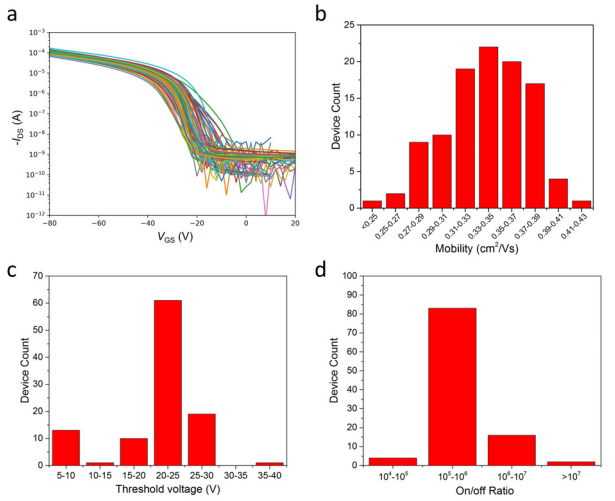

Figure S10| Statistics of the polymer FET performance on SiO_2/Si substrate. 105 devices were measured from 5 substrates. The devices have channel lengths of 50 μm and channel width of 1000 μm. The applied gate voltage is from +20 to −80 V and drain-source voltage is −80 V. The average mobility is 0.34 ± 0.04 cm^2/Vs. The average threshold voltage is 21.0 ± 6.1 V.

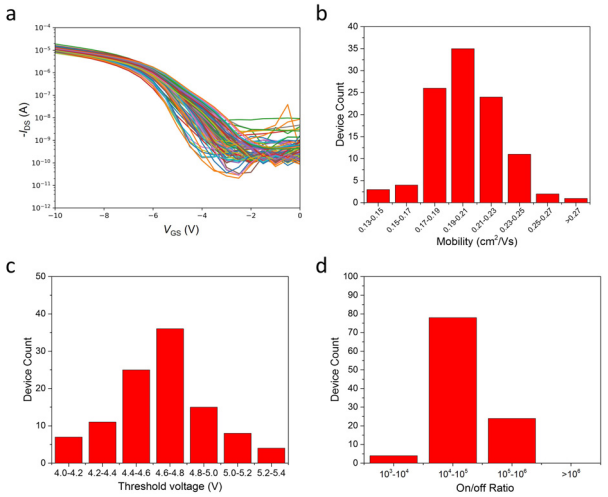

Figure S11| Statistics of the polymer FET performance on Al_2O_3 dielectric. 106 devices were measured from 5 substrates. The devices have channel lengths of 50 μm and channel width of 1000 μm. The applied gate voltage is from 0 to −10 V and drain-source voltage is −10 V. The average mobility is 0.21 ± 0.03 cm^2/Vs. The average threshold voltage is 4.67 ± 0.28 V.

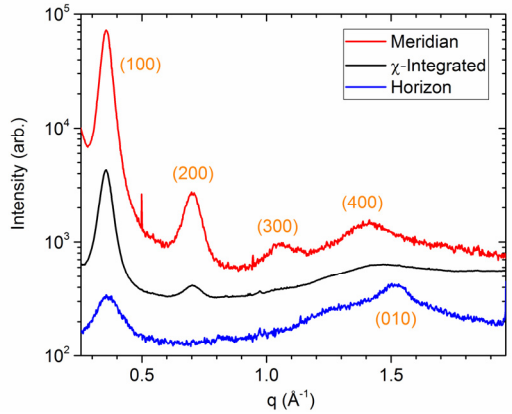

Figure S12| Line cuts of the 2D-GIXD pattern of PDPP-PD film. The lamella peaks (*h*00) appear mainly in the meridian direction while the π- π stacking peak appears the horizon direction, indicating an edge-on polymer packing is preferred.

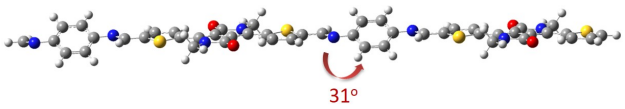

Figure S13| Optimized polymer structure of PDPP-PD. The polymer shows a dihedral angle of 31° due to the repulsive interaction between the imine bond and the benzene ring. This dihedral angle is larger than other DPP based polymers (0-10°),[5] resulting in a larger π- π stacking distance.

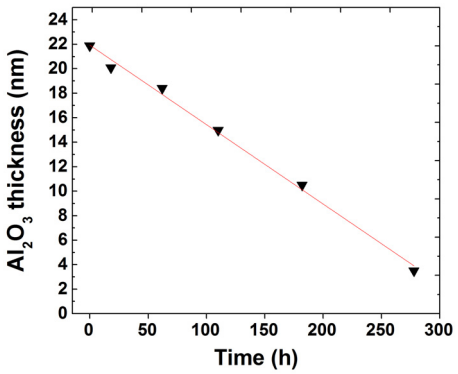

Figure S14| Disintegration of the ALD-deposited Al_2O_3 layer. Film thickness changes of an ALD Al_2O_3 layer in a pH-4.6 buffer solution. The film thickness is measured by ellipsometer, showing a linear decomposition speed of 1.5 nm/day.

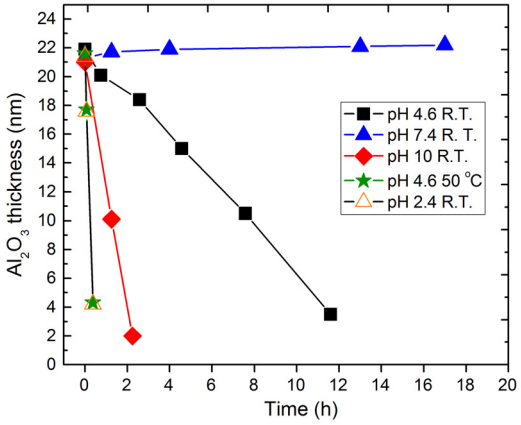

Figure S15| Disintegration of the ALD-deposited Al_2O_3 layer in different pH at room temperature (22 °C) or at a higher temperature. The Al_2O_3 is stable in pH=7.4 PBS buffer solution. However, more basic and acidic solutions or higher temperature lead to faster disintegration of the Al_2O_3.

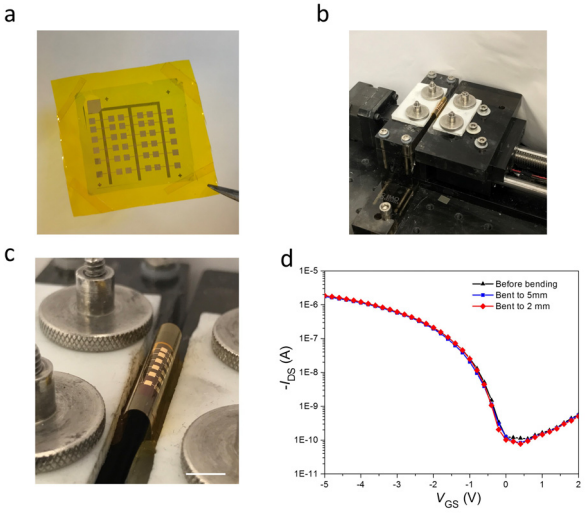

Figure S16| Bending test of the disintegrable device. a, After dissolving the sacrificial layer, an ultrathin device was transferred onto a 25 μm polyimide substrate for bending test. **b** and **c**, Photos of our home-built bending test station. The device was bent to a radius of ≈2 mm. Scale bar: 5 mm. **d**, Transfer characteristics of a device before and after bending at different radii of curvatures (V_{DS} = −5 V).

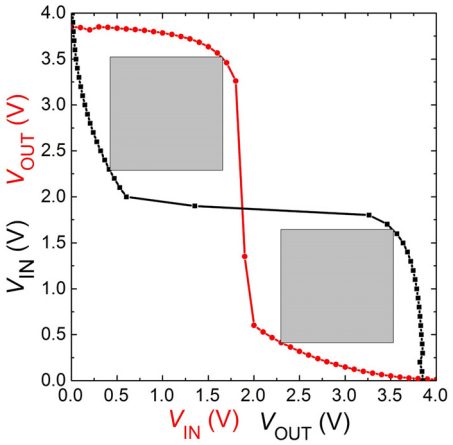

Figure S17| Noise margin calculation of a pseudo-D inverter. The noise margin of the inverter was calculated by determining the maximum size of a square fit between inverter curve and its mirrored curve.[6]

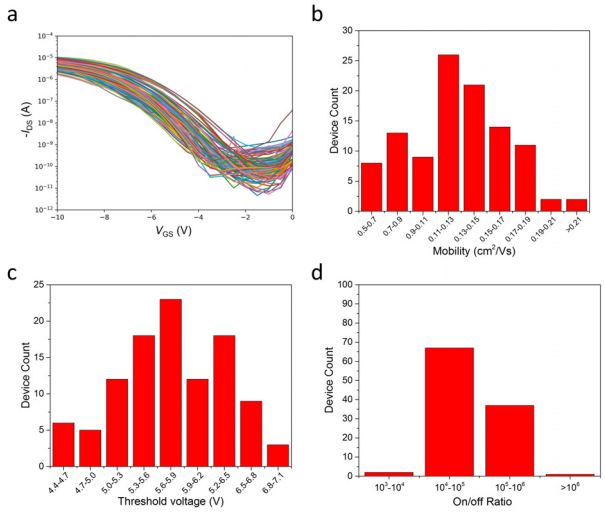

Figure S18| Statistics of the polymer FET performance on Al_2O_3 dielectric using Fe as source-drain electrodes. 107 devices were measured from 5 substrates. The devices have channel lengths of 50 μm and channel width of 1000 μm. The applied gate voltage is from 0 to −10 V and drain-source voltage is −10 V. The average mobility is 0.12 ± 0.04 cm^2/Vs. The average threshold voltage is 5.75 ± 0.61 V.

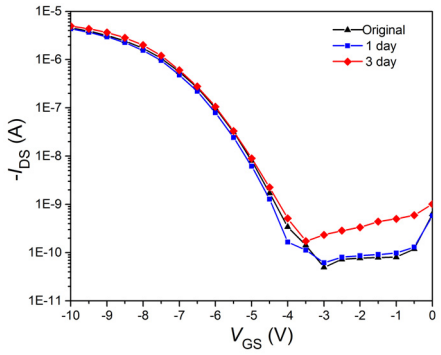

Figure S19| Transfer characteristic changes of a device before and after soaking in DI water for 1 day and 3 days. The transfer curves indicate that the device performance did not show significant changes after soaking in DI water. The device was fabricated on Al_2O_3 dielectric layer (25 nm) with Fe as source-drain electrodes (L = 50 μm, W = 1000 μm). The applied gate voltage is from 0 to −10 V and drain-source voltage is −10 V.

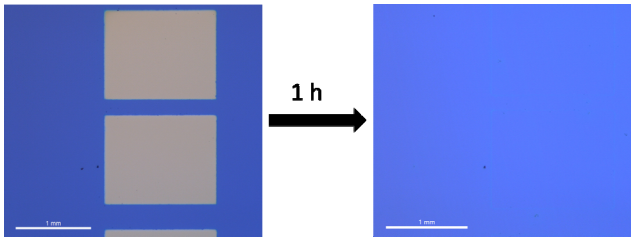

Figure S20| Disintegration of iron electrodes in a pH=4.6 buffer solution. The iron electrodes were evaporated on SiO_2/Si substrates. The electrodes disappeared completely after 1 h of soaking in the buffer solution.

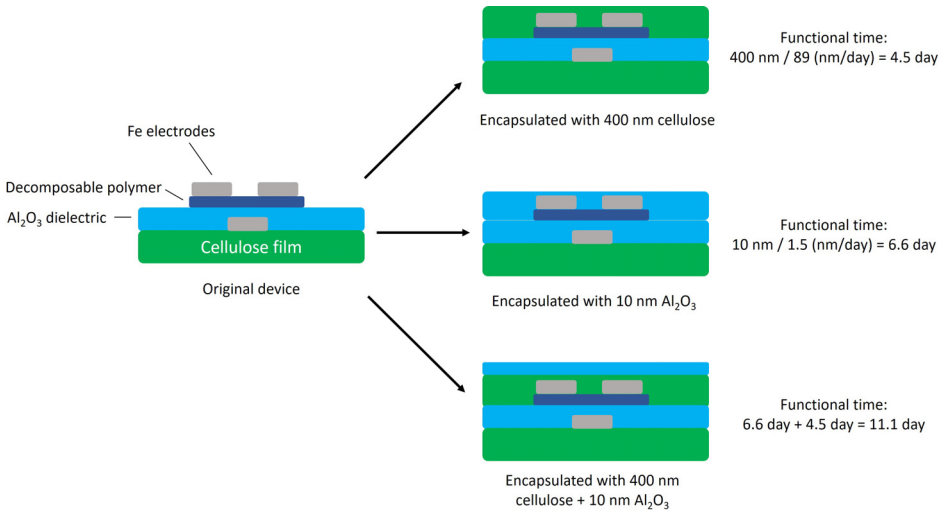

Figure S21| Proposed strategy to control of the degradation speed of the device using decomposable polymer or metal oxide as the encapsulation materials. The functional time period of the device can be determined by the thickness and the degradation speed of the encapsulation layer, because the devices stop functioning as soon as the acidic solution meets the iron electrodes. At pH 4.6, the cellulose film has a degradation speed of 3.7 nm/h (89 nm/day) and the Al_2O_3 has a degradation speed of 1.5 nm/day at room temperature (22 °C).

Table S1. Thickness, density, weight percentage, and toxicity of the materials used in the device.

Materials	Thickness (nm)	Density (g/cm^3)	Mass for a 1 cm^2 device (μg)	Weight percentage (%)	Toxic components
Cellulose	800	1.5	120	60	non-toxic
Fe	80	7.9	63	32	non-toxic
Al_2O_3	25	3.9	9.8	4.9	Al^{3+}(5.2 μg/cm^2) [b]
PDPP-PD	40	1.1[a]	4.4	4.2	PPD (0.48 μg/cm^2)[c] DPP (3.92 μg/cm^2)[d]
Total	945	–	190	100	–

(a) Density of the conjugated polymer is in the range from 0.9 to 1.1 g/cm^3, estimated from refercence.[7]
(b) For drinking water, the recommended Secondary Maximum Contaminant Level (SMCL) for aluminum is 0.05-0.2 mg/L.[8] This means that the intake amount of Al from a 1-cm^2 device is no more than 2.5–100 mL drinking water.
(c) *p*-Phenylenediamine (PPD) is permitted by the FDA for use as a hair dye.[9] The LD50 of PPD is 80 mg/kg (rats). The amount of the PPD in a 1-cm^2 device is much lower than this value.
(d) Toxicity study shows that short-term inhalation of DPP pigments (6 h/day on 5 consecutive days) with high dose (30 mg/m^3) only caused minor effects on the lungs. No expected ecotoxicological threats to human health and the environment were observed for DPP dyes used for tattoos.[10]

REFERENCES

(1) Li, Y. US Pat. Application 2009/65766 A1 and 2009/0065878 A1, 2009.

(2) Kim, J. H.; Kim, K. H.; Lee, D. H.; Yang, D. S.; Heo, D. U.; Lee, T. W.; Cho, M. J.; Choi, D. H. *Mol. Cryst. Liq. Cryst.* **2013**, *581*, 38.

(3) Kontturi, E.; Thüne, P. C.; Niemantsverdriet, J. W. *Polymer* **2003**, *44*, 3621.

(4) Gaussian 09, Revision D.01, M. J. Frisch, G. W. Trucks, H. B. Schlegel, G. E. Scuseria, M. A. Robb, J. R. Cheeseman, G. Scalmani, V. Barone, B. Mennucci, G. A. Petersson, H. Nakatsuji, M. Caricato, X. Li, H. P. Hratchian, A. F. Izmaylov, J. Bloino, G. Zheng, J. L. Sonnenberg, M. Hada, M. Ehara, K. Toyota, R. Fukuda, J. Hasegawa, M. Ishida, T. Nakajima, Y. Honda, O. Kitao, H. Nakai, T. Vreven, J. A. Montgomery, Jr., J. E. Peralta, F. Ogliaro, M. Bearpark, J. J. Heyd, E. Brothers, K. N. Kudin, V. N. Staroverov, T. Keith, R. Kobayashi, J. Normand, K. Raghavachari, A. Rendell, J. C. Burant, S. S. Iyengar, J. Tomasi, M. Cossi, N. Rega, J. M. Millam, M. Klene, J. E. Knox, J. B. Cross, V. Bakken, C. Adamo, J. Jaramillo, R. Gomperts, R. E. Stratmann, O. Yazyev, A. J. Austin, R. Cammi, C. Pomelli, J. W. Ochterski, R. L. Martin, K. Morokuma, V. G. Zakrzewski, G. A. Voth, P. Salvador, J. J. Dannenberg, S. Dapprich, A. D. Daniels, O. Farkas, J. B. Foresman, J. V. Ortiz, J. Cioslowski, and D. J. Fox, Gaussian, Inc., Wallingford CT, 2013.

(5) Nielsen, C. B.; Turbiez, M.; McCulloch, I. *Adv. Mater.* **2013**, *25*, 1859.

(6) Gelinck, G.; Heremans, P.; Nomoto, K.; Anthopoulos, T. D. *Adv. Mater.* **2010**, *22*, 3778.

(7) Machui, F.; Rathgeber, S.; Li, N.; Ameri, T.; Brabec, C. J. *J. Mater. Chem.* **2012**, *22*, 15570.

(8) Public Health Statement of Aluminum https://www.atsdr.cdc.gov/toxprofiles/tp22-c1.pdf accessed on Nov. 6, 2016.

(9) http://www.fda.gov/Cosmetics/ProductsIngredients/Products/ucm108569.htm accessed on Nov. 6, 2016

(10) (a) Hofmann, T.; Ma-Hock, L.; Strauss, V.; Treumann, S.; Rey Moreno, M.; Neubauer, N.; Wohlleben, W.; Gröters, S.; Wiench, K.; Veith, U.; Teubner, W.; van Ravenzwaay, B.; Landsiedel, R. *Inhal. Toxicol.* **2016**, *28*, 463; (b) Petersen, H.; Lewe, D. *Curr. Probl. Dermatol.* **2015**, *48*, 136.